Effect of Turbulence Length Scale on Vortex Induced Vibration of Twin Deck Bridge Section

*Ralph Acebedo[1)], Sang-Won Kim[2)], You-Chan Hwang[3)] and Ho-Kyung Kim[4)]

[1), 2), 3), 4)] Department of Civil and Environmental Engineering,
Seoul National University, Seoul, Gwanak-gu, South Korea
[1)] ralphacebed@snu.ac.kr

ABSTRACT

The effect of turbulence scale on the vortex induced vibration of a twin deck bridge section was evaluated by wind tunnel experiment. The bridge section that was utilized in the experiment was a 1/100 scale model based on an actual twin deck bridge section and target wind power spectra was generated based on actual topographic condition. Several wind turbulence conditions were generated by the use of active turbulence generator (ATG). At lock-in wind speed, the root-mean-square (RMS) amplitudes of the vortex-induced vibration (VIV) of the bridge section were determined under laminar condition and at different turbulent wind conditions. Experimental data showed that for the given twin-deck section, turbulent wind decreased the RMS amplitude of the VIV. As turbulence intensity increased, RMS amplitude decreased. However for a given constant intensity, the turbulence length scale had no effect on the VIV RMS amplitude.

1. INTRODUCTION

For slender and flexible structures such as long span bridges, the natural frequency and the damping are relatively small which make these structures susceptible to vortex-induced induced vibrations when subjected to wind. As air flows past the bridge deck at given velocities, it causes alternating vortices to form at a certain frequency. Vortex-induced vibration (VIV) occurs when vortex-shedding frequency and bridge's natural frequency are approximately the same.

The vortex-induced vibration of bridges are well investigated and demonstrated in the wind tunnel tests typically at laminar flow. Past studies illustrated that for most sections, the VIV is at maximum at laminar flow (M, Kawatani, et al. 1992, 1993). For a wind tunnel test, subjecting a bridge section under a laminar flow will most likely give

[1)] Master Student
[2), 3)] PhD Student
[4)] Professor

conservative results. However it is important to understand and illustrate the aerodynamic behavior of the bridge section under the natural wind that is a turbulent wind flow.

Wind turbulence is the fluctuation and seemingly random motion of air. It is expressed in terms of turbulence spectra with two parameters: the turbulence intensity and the integral length. The effects of turbulent flows on vortex-induced vibration of several sections were well illustrated by previous researches most of them focused on changing of turbulence intensities only since controlling the length scale was not easy. However, researches done by M. Kawatani, et al, 1992, 1993 illustrated the VIV of different single deck sections under turbulent wind not only with varying turbulence intensity but also with varying turbulence length scale. The purpose of this study is to reinforce previous researches by testing the VIV of a twin-deck bridge section under turbulent wind with varying length scale.

2. THEORETICAL BACKGROUND

Wind turbulence is expressed in turbulence spectra, and it has two parameters, the turbulence intensity and the integral length scale. Turbulence intensity is the standard deviation of the wind speed component divided by average wind speed over some time period. While the turbulence length scale is the product of average velocity and integral time scale. The turbulence length scale is a physical quantity describing the size of the large energy-containing eddies.

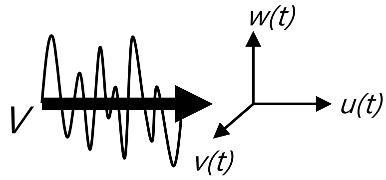

Fig. 1 Wind Component

The auto covariance functions and corresponding auto covariance coefficients of a wind signal are defined by

$$Cov_n(\tau) = E\left[n(t)n(t+\tau)\right] = \frac{1}{T}\int_0^T n(t)n(t+\tau)dt \tag{1}$$

$$\rho_n(\tau) = \frac{Cov_n(\tau)}{\sigma_n^2} \qquad \text{where } n = u, v, w \tag{2}$$

where τ is an arbitrary time lag.

The time scale may be interpreted as the average duration of a *u*, *v* or *w* wind gust.

$$T_n = \int_0^\infty \rho_n(\tau)d\tau \qquad \text{where } n = u, v, w \tag{3}$$

The corresponding length scale

$$L_n = V \times \int_0^\infty \rho_n(\tau) d\tau \qquad \text{where } n = u, v, w \tag{4}$$

Spectral densities represents the frequency properties for the turbulence components. For this study, Von Karman Spectra is utilized.

$$\frac{f \times S_n(f)}{\sigma_n^2} = \frac{4 \times \hat{f}_n \times \left(1 + 755.2 \times \hat{f}_n^2\right)}{\left(1 + 283.2 \times \hat{f}_n^2\right)^{11/6}} \tag{5}$$

$$\hat{f}_n = f \times L_n / V \qquad \text{where } n = v, w \tag{6}$$

where $S_n(f)$ is the autospectral density function and $\hat{f}_n$ is a non-dimensional frequency.

3. TURBULENCE WIND GENERATION

The generation of wind was performed in Seoul National University's (SNU) two-dimensional wind tunnel facility. The wind tunnel test section is 1.0 meter in width, 1.5 meters in height and 4.0 meters in length and has wind speed range of 0.5m/s~20.0m/s. Wind turbulences can be generated in a wind tunnel by two different ways, i.e. an active method using a turbulence generator and a passive method using a grid.

Fig. 2 Seoul National University wind tunnel facility

3.1. Active Turbulence Generator

An active turbulence generator (ATG) is composed of active plates and airfoils driven by motor. They move in seemingly random but in calculated manner. ATG is very effective in producing wind turbulence with target intensity, length scale and spectra. However the procedure is not straight forward as it is in grid.

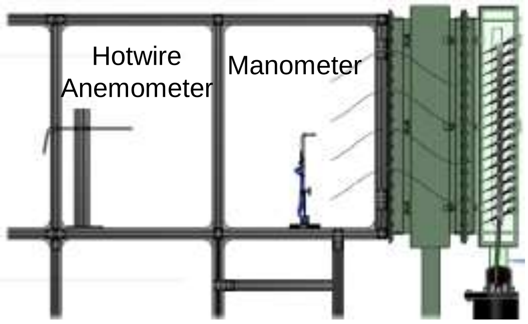

Fig. 3 ATG set-up

In generating wind turbulence using ATG, the target power spectra was predetermined. The wind velocity at which peak amplitude VIV occurred was determined by preliminary tests. Target turbulence intensity and turbulent length scales were calculated based on on-site topographic conditions and with the use of Von Karman spectra (eqn 5), a target curve was generated. The target spectral density was converted into simulated wind time history. This procedure involved randomized phase angle so given same power spectrum could have infinite number of different simulated wind.

The generated time history was then converted into motor angle for airfoils. After the motor signal was inputed into ATG, wind time history was measured and consequently the power spectral density was calculated and compared to the target spectra. Initial calculations had different values to the target. To match the wind signal spectra to target spectra, a modification factor was multiplied to the signal. The resulting spectra was converted back to time domain as the modified wind signal by inverse Fast Fourier Transform (FFT). It was again converted into motor angle and new measurements were gathered. The whole process was repeated until the wind signal spectra matched with the target.

In this study, winds were generated with different turbulence properties. The first set of wind was with constant turbulence intensity and various turbulence length scale (see Table 1), and another set was with constant turbulence length scale and different turbulence intensity (see Table 2). The values for these parameters were based on the on-site conditions. The turbulence intensity range was around 3.5% to 8.2% while the vertical turbulence length scale was around 3.5m to 40m (0.035m to 0.400m in wind tunnel).

Table 1 ATG Generated Wind – Varying Turbulence Length Scale

Wind Name	U (m/s)	Iw (%)	Lx,w (m)
ATG-Lw-40	2.10	6.4	4.0
ATG-Lw-80			8.0
ATG-Lw-130			13.0
ATG-Lw-165			16.5
ATG-Lw-270			27.0
ATG-Lw-330			33.0
ATG-Lw-400			40.0

Table 2 ATG Generated Wind – Varying Turbulence Intensity

Wind Name	U (m/s)	Iw (%)	Lx,w (m)
ATG-Iw-5.2	2.10	5.2	13.0
ATG-Iw-6.4		6.4	
ATG-Iw-8.2		8.2	

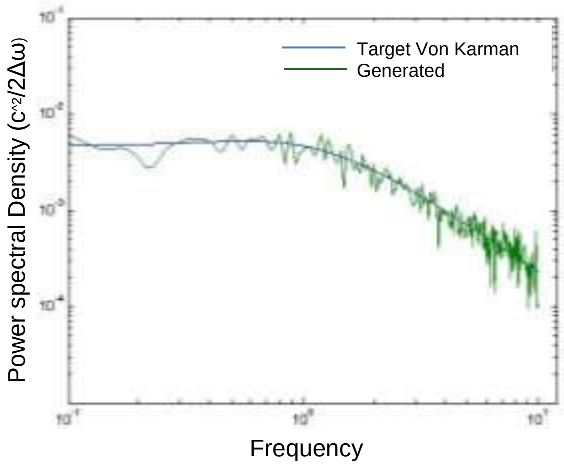

Fig. 4 Spectral Density of Turbulent Wind (ATG-Iw-6.4)

3.2. Grid Turbulence

The grid-generated turbulences have been conveniently utilized in many cases by simulating various levels of turbulence intensities. The dominant factors affecting the generated turbulence intensities are the size of grid elements, gap distance between elements and the distance of the testing point from the grid. Although the target turbulent intensity is achievable, the target turbulent length scale and spectra is almost impossible to satisfy all the time.

For the purpose of showing the effects of turbulence produced by grid on VIV, three grid set-up were performed. The target frequency for this study is from 0.1Hz to 10Hz.

Table 3. Grid Generated Turbulence

Grid		Target		Measured	
	U (m/s)	Iw (%)	Lx,w (m)	Iw (%)	Lx,w (m)
Grid-Iw-3.5	2.10	3.5	13.0	3.8	1.5
Grid-Iw-6.4		6.4		6.6	1.6
Grid-Iw-7.5		7.5		7.3	2.1

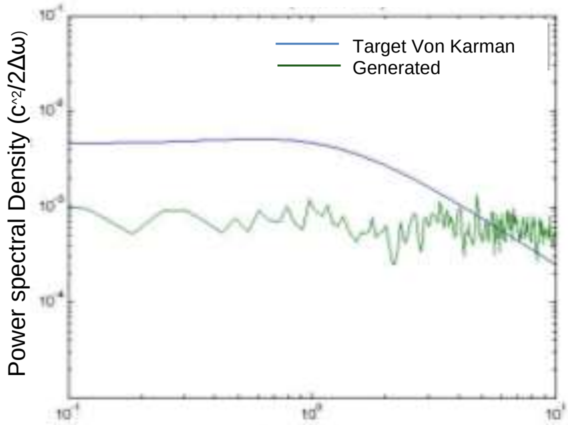

Fig. 5 Spectral Density of Turbulent Wind (Grid-Iw-6.4)

4. EXPERIMENTAL SET-UP

The target bridge deck was a twin deck bridge section and was based on the initial section of an actual bridge. The initial section of the bridge demonstrated significant VIV. However the final section of the bridge were sufficiently modified to suppress the unwanted vibration.

The section model was made of balsa with the scale of 1/100. The model dimension were: 0.900meter length, 0.410meter width and 0.040meter depth. The section model was mounted on a spring-support system with equivalent measured vertical frequency equal to 5.896Hz. The first vertical mode of the prototype was 0.64Hz which consequently resulted to a timescale value of 9.15.

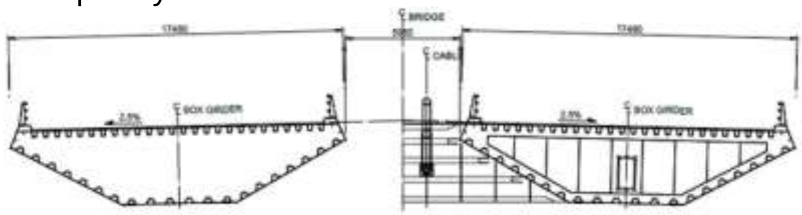

Fig. 6 Deck Section

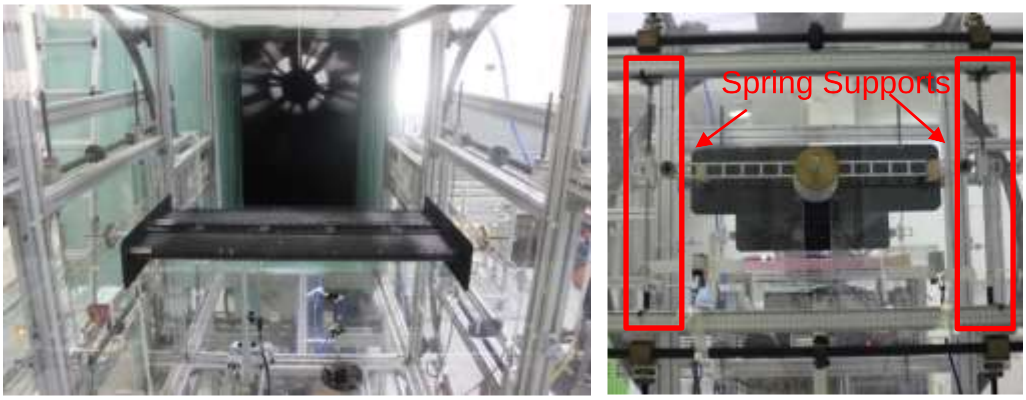

Fig. 7 Section model set up

5. RESULTS

5.1 Wind Turbulence with Different Turbulence Length Scales (by ATG)

The bridge deck model was first subjected to laminar flow (Iw~<0.8%). The bridge response was measured by its root mean square of the amplitudes. The bridge model was then subjected to wind turbulence under ATG winds (see Table 1) and the results were overlaid on each other. The turbulence intensity was set to 6.4% while vertical turbulence length scale range was from 4m to 40m. The ratio of maximum RMS amplitude under turbulent condition of ATG and the peak RMS of laminar flow was also computed.

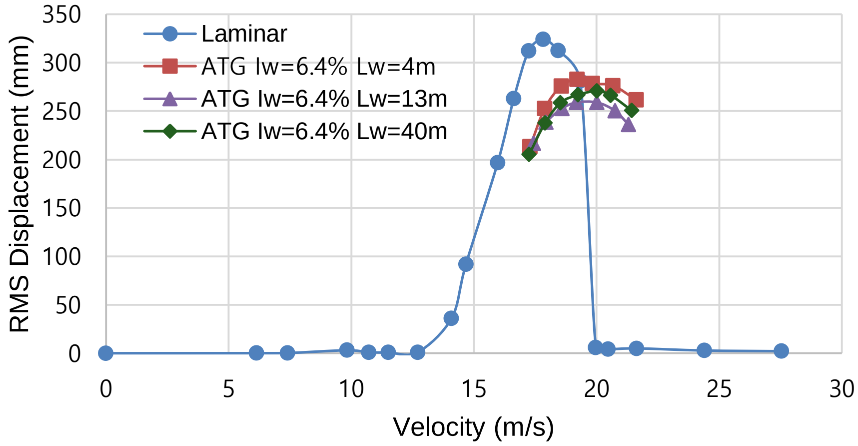

Fig. 8 Velocity – Displacement Amplitude (RMS)

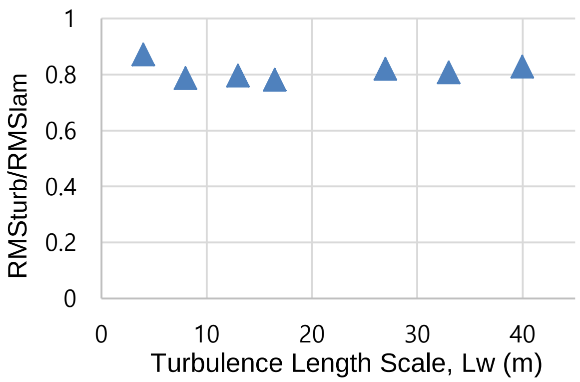

Fig. 9 Response Ratio under Different Turbulent Length Scales

Wind tunnel experiment results show that the velocity at which peak point for VIV occurred under turbulent condition moved to higher velocity as compared to laminar condition. Also, as turbulent length scale is increased, the response seems to have no trend and remained around 80% of that of the laminar. The turbulence length scale seems to have no effect on the response of the bridge.

5.2 Wind Turbulence with Different Wind Signals (by ATG)

In the ATG wind generation procedure, converting the target spectrum into simulated wind included a random phase angle. Therefore a single target spectrum could have infinite number of simulated wind. The bridge was tested under the same turbulent spectrum i.e. same turbulence intensity, 6.4%, and turbulence length scale, 13.0m, but with different random seeds. The bridge response show almost no changes in the response amplitude for different wind signal. This is not surprising result since all of the four winds correspond to the same spectral density. The randomness of the wind signal does not affect the response of the bridge.

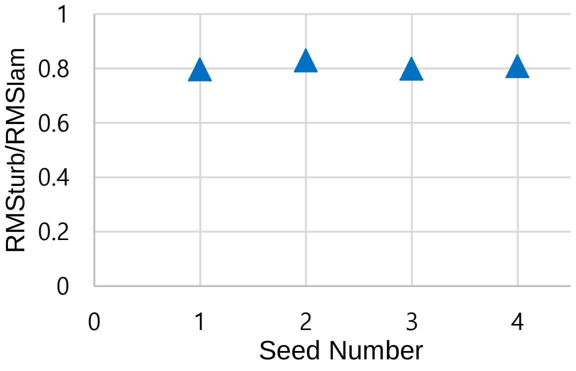

Fig. 10 Response Ratio under Different Wind Signals

5.3 Wind Turbulence with Different Turbulence Intensities (by ATG)

The bridge was tested under turbulent wind with different turbulence intensities by the use of ATG (see Table 2). The turbulence intensities were at 5.2%, 6.4% and 8.2% while the turbulence length scale was set at 13.0m. In Fig 11, the bridge response shows as turbulence intensity is increased, bridge response amplitude is decreased.

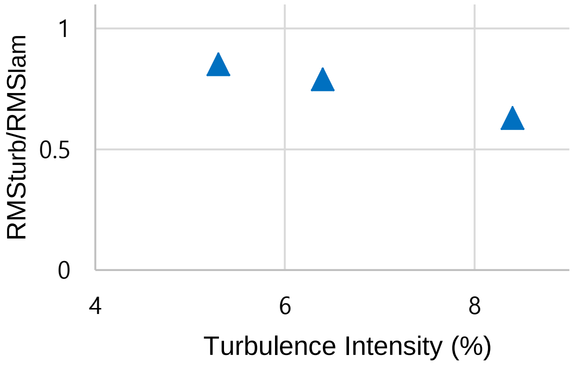

Fig. 11 Response Ratio under Different Turbulent Intensities (ATG)

5.4 Wind Turbulence with Different Turbulence Intensities (by Grid)

Similarly, the bridge model was tested under different turbulence intensities by use of Grid (see Table 3). The results show similar downward trend as the intensity values is increased.

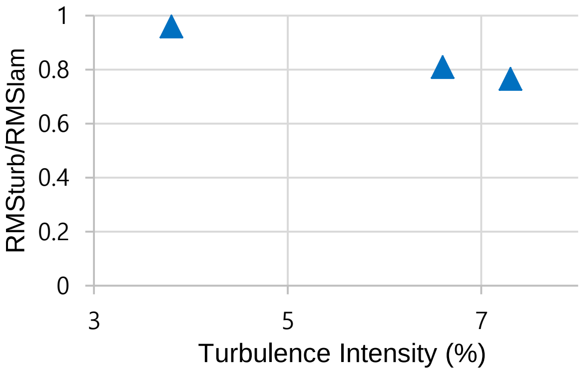

Fig. 12 Response Ratio under Different Turbulent Intensities (GRID)

In part 5.4, the bridge was tested under winds generated by grid. In using grid, it can only achieve the target turbulence intensity. The effects of turbulence length scale is neglected every time a grid is utilized. However, results in part 5.1 suggest that turbulence length scale is a non-factor, therefore the results in part 5.3 and part 5.4 should have similar values.

In Figure 13, the results of parts 5.3 and 5.4 were merged. The two have different turbulence length scale, however they have similar trend. At turbulence intensity around 6.4%, the responses for grid and ATG have almost the same amplitude.

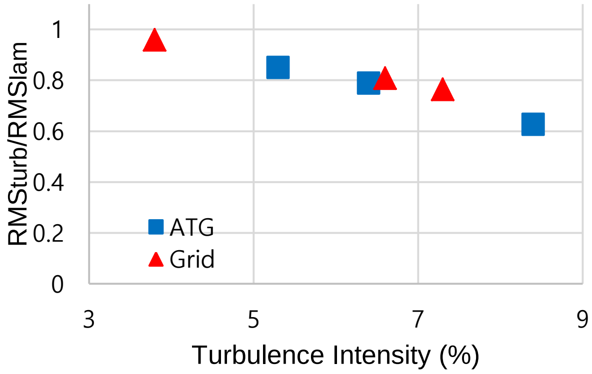

Fig. 13 Response Ratio under Different Turbulent Intensities

3. CONCLUSIONS

Based on the experimental results conducted in the wind tunnel, the following conclusions can be drawn:

-The vortex-induced vibration response amplitude of the bridge section under turbulent condition decreased as compared to that under laminar condition. In addition, the location of peak amplitude moved to higher velocity.

-Turbulence length scale had no direct effect on the VIV displacement response of the bridge.

-Vortex-induced vibration was highly influenced by the turbulence intensity. As turbulence intensity was increased, response amplitude decreased.

-VIV response amplitude was not affected by the randomness of the wind signal.

REFERENCES

Kobayashi, H., Kawatani, M., Kim, H. (1992). “Effects of Turbulence Characteristics on Vortex-Induced Oscillation of Rectangular Cylinders”. Journal of Wind Engineering and Industrial Aerodynamics, **41-44**, 775-784

Kawatani, M., Kim, H., Uejima, H., Kobayashi, H. (1993). “Effects of Turbulent Flows on Vortex-Induced Oscillation of Bridge Girders with Basic Sections”. Journal of Wind Engineering and Industrial Aerodynamics, **49**, 477-486

Burton, T., Sharpe, D., Jenkins, N. and Bossanyi, E. (2001), “Wind Energy Handbook”, John Wiley & Sons Ltd, p23

Honshu-Shikoku Bridge Expressway Authority, (2001), “Design Guidelines for Honshu-Shikoku Bridge Expressway”

So, R.M.C., Wang, X.Q., Xie, W.C., Zhu, J. (2008), “Free-stream turbulence effects on vortex-induced vibration and flow-induced force of an elastic cylinder”. Journal of Fluids and Structures. Vol 24, Issue 4, 481-495

Strommen, E. (2010), “Theory of Bridge Aerodynamics”, Springer-Verlag

Daniels, S., Castro, I., Xie, Z.T. (2015), “Numerical analysis of freestream turbulence effects on the vortex-induced vibrations of a rectangular cylinder”. J. Wind Eng. Ind. Aerodyn. **153** (2016) 13-25

Daniels, S., Xie, Z.T. (2015). “Free-Stream Turbulence Effects on Long-Span Bridge Aerodynamics”. 7th International Conference on Fluid Mechanics, ICFM7

Hwang, Y.C., Han, S.W., Kim, H.K. (2016), “Mitigation of vertical vortex-induced vibration for a twin box girder by inspection rails”